The EMBO Journal (2010) 29, 3484–3495 | © 2010 European Molecular Biology Organization | All Rights Reserved 0261-4189/10
www.embojournal.org

THE EMBO JOURNAL

Differences in signalling by directly and indirectly binding ligands in bacterial chemotaxis

Silke Neumann[1], Clinton H Hansen[2,3], Ned S Wingreen[2,*] and Victor Sourjik[1,*]

[1]Zentrum für Molekulare Biologie der Universität Heidelberg, DKFZ-ZMBH Alliance, Heidelberg, Germany and [2]Department of Molecular Biology, Princeton University, Princeton, NJ, USA

In chemotaxis of *Escherichia coli* and other bacteria, extracellular stimuli are perceived by transmembrane receptors that bind their ligands either directly, or indirectly through periplasmic-binding proteins (BPs). As BPs are also involved in ligand uptake, they provide a link between chemotaxis and nutrient utilization by cells. However, signalling by indirectly binding ligands remains much less understood than signalling by directly binding ligands. Here, we compared intracellular responses mediated by both types of ligands and developed a new mathematical model for signalling by indirectly binding ligands. We show that indirect binding allows cells to better control sensitivity to specific ligands in response to their nutrient environment and to coordinate chemotaxis with ligand transport, but at the cost of the dynamic range being much narrower than for directly binding ligands. We further demonstrate that signal integration by the chemosensory complexes does not depend on the type of ligand. Overall, our data suggest that the distinction between signalling by directly and indirectly binding ligands is more physiologically important than the traditional distinction between high- and low-abundance receptors.

The EMBO Journal (2010) **29,** 3484–3495. doi:10.1038/emboj.2010.224; Published online 10 September 2010
Subject Categories: signal transduction; microbiology & pathogens
Keywords: bacterial chemotaxis; FRET; signal integration; signal transduction; transport

Introduction

Chemotactic bacteria follow chemical gradients in their environment by performing temporal comparisons of chemoeffector concentrations (Berg and Brown, 1972; Macnab and Koshland, 1972). In *Escherichia coli*, sensing and processing of stimuli are performed by complexes that consist of four types of attractant-specific chemoreceptors, a histidine kinase CheA, and an adaptor protein CheW (Gegner *et al*, 1992). Attractant binding to the periplasmic part of a receptor homodimer, the functional chemoreceptor unit—hereafter simply referred to as a 'receptor'—inhibits CheA autophosphorylation, thus reducing phosphotransfer to the motor regulator CheY. The signal transduction pathway also includes a phosphatase CheZ, and an adaptation system that consists of a methyltransferase, CheR, and a methylesterase, CheB. Adaptation to a persistent attractant stimulus works through receptor methylation on four specific glutamate residues, which increases CheA activity and decreases sensitivity to the attractant (Borkovich *et al*, 1992; Li and Weis, 2000; Levit and Stock, 2002).

Although all *E. coli* chemoreceptors are homologous, two classes of ligands can be distinguished based on their binding properties. Amino acids bind directly to the periplasmic domains of the so-called major receptors Tar and Tsr, and constitute one class. A second class is represented by sugars and dipeptides, which bind to minor receptors Trg and Tap, respectively, through periplasmic substrate-binding proteins (BPs) of ATP-binding cassette (ABC) transporters. An interesting exception is the sugar maltose, which binds indirectly to the major receptor Tar (Hazelbauer, 1975; Manson and Kossmann, 1986). Early studies of chemotaxis that relied on accumulation of bacteria into attractant-filled microcapillaries already indicated differences in the magnitude and concentration range of responses mediated by the two types of ligands (Mesibov and Adler, 1972; Adler *et al*, 1973; Mesibov *et al*, 1973), but the origin of those differences remained largely unclear.

Apart from the mode of ligand binding, major and minor receptors differ in their copy numbers, with the total number of minor receptors previously estimated to be <1000 copies per cell compared with $\sim 10\,000$ for major receptors (Li and Hazelbauer, 2004), and this difference was frequently assumed to explain the apparently weaker responses mediated by minor receptors. Yet another difference lies in the truncation for the minor receptors of the last 20 amino acids of the C-terminus, which includes the binding site for the adaptation enzymes, making minor receptors dependent on the proximity of neighbouring major receptors for efficient adaptation (Li and Hazelbauer, 2005).

The receptor–kinase sensory complexes are organized in large clusters that localize at the cell poles and in smaller clusters along the cell body (Maddock and Shapiro, 1993; Sourjik and Berg, 2000), where receptors of different ligand specificities are intermixed (Ames *et al*, 2002). Activities of neighbouring receptors are allosterically coupled, resulting in amplification of receptor-mediated stimuli (Li and Weis, 2000; Gestwicki and Kiessling, 2002; Sourjik and Berg, 2002, 2004; Lai *et al*, 2005), and thus allowing *E. coli* to generate highly sensitive responses that approach physical limits of sensitivity (Berg and Purcell, 1977; Bialek and Setayeshgar, 2005). The allosteric interactions between

*Corresponding authors. NS Wingreen, Department of Molecular Biology, Princeton University, Princeton, NJ 08544-1014, USA. Tel.: +1 609 258 8476; Fax +1 609 258 8616; E-mail: wingreen@princeton.edu or
V Sourjik, Zentrum für Molekulare Biologie der Universität Heidelberg, Im Neuenheimer Feld 282, Heidelberg 69120, Germany.
Tel.: +49 6221 54 6858; Fax: +49 6221 54 5894;
E-mail: v.sourjik@zmbh.uni-heidelberg.de
[3]Present address: Biophysics Program, Harvard University, Cambridge, MA 02138, USA

Received: 17 March 2010; accepted: 16 August 2010; published online: 10 September 2010

receptors have been described using a number of mathematical models (Bray *et al*, 1998; Duke *et al*, 2001; Sourjik and Berg, 2004; Mello and Tu, 2005; Keymer *et al*, 2006). The most commonly applied are Monod–Wyman–Changeux type (MWC) models, which assume that receptors within clusters exist in tightly coupled allosteric signalling complexes, or teams, of 10–20 receptors, with all receptors in one team switching synchronously between inactive (*off*) and active (*on*) states (Sourjik and Berg, 2004; Mello and Tu, 2005; Keymer *et al*, 2006). As receptors of different types are intermixed within clusters (Ames *et al*, 2002), allosteric interactions between receptors also provide a means of signal integration (Sourjik and Berg, 2004).

So far, most of the effort to investigate signal processing by allosteric chemoreceptor teams has concentrated on the directly binding ligands of the major receptors Tar and Tsr, L-aspartate (or its non-metabolizable analogue α-methyl-DL-aspartate, MeAsp) and L-serine (or its non-metabolizable analogue α-aminoisobutyrate, AiBu), respectively. The goal of this work was to systematically compare intracellular signalling by the directly binding ligands of major receptors with that mediated by the indirectly binding sugars D-maltose (specific for Tar), D-ribose and D-galactose (specific for Trg), and the dipeptide Pro-Leu (specific for Tap). To quantify signalling parameters of individual ligands, we determined relative expression levels of the corresponding receptors and extended the MWC model of allosteric teams to describe indirect ligand binding through BPs. Our results show that the signalling strength and dynamic range of a specific ligand are determined both by its binding properties and by the expression levels of its receptor and the respective BP. We conclude that the indirect mode of ligand binding allows greater flexibility in the modulation of response sensitivity, but at a cost of a narrower dynamic range. Chemotactic response to mixtures of effectors showed that simultaneous stimulation by ligands of different receptors is additive, and that adaptation to ligands of one receptor does not interfere with signalling by other receptors. On the basis of these and other data, we discuss possible evolutionary origins of the two modes of ligand binding in relation to strategies of coupling between chemotaxis and transport.

Results

Responses towards directly and indirectly binding ligands

To measure intracellular responses, we used a FRET reporter based on the CheY-YFP/CheZ-CFP pair (Sourjik and Berg, 2002; Sourjik *et al*, 2007). The FRET assay determines the relative intracellular level of the complex formed by phosphorylated CheY-YFP and CheZ-CFP. As the amount of this complex is proportional to the rate of CheY phosphorylation, it provides a direct readout of the intracellular kinase activity (Supplementary Figure S1). It has been shown before that CheY-YFP/CheZ-CFP FRET changes linearly with the kinase activity within the physiological activity range (Sourjik and Berg, 2002; Sourjik *et al*, 2007; Endres *et al*, 2008). As wild type for our experiments, we used a *cheY cheZ* derivative of *E. coli* K-12 strain LJ110 (Zeppenfeld *et al*, 2000) whose parent W3110 was used for early studies on sugar taxis (Hazelbauer *et al*, 1969; Adler *et al*, 1973). This strain shows saturating expression of galactose BP (GBP) (see below), which makes it convenient for comparative study of amino acid and sugar taxis.

When pre-adapted in buffer before stimulation, wild-type cells responded to the natural ligands of major and minor receptors in a similar concentration range, with EC_{50} values—the ligand concentrations at the half-maximal response—being 193 and 126 nM for the Tar ligands aspartate and maltose, respectively, 165 nM for the Tsr ligand serine, 15 and 63 nM for the Trg ligands galactose and ribose, respectively, and 356 nM for the dipeptide Pro-Leu, a ligand of Tap (Figure 1A and B). Lower sensitivity was observed for the response to the non-metabolizable ligands of Tar (MeAsp) and of Tsr (AiBu), with EC_{50} values of 2.2 and 48 μM, respectively. Response amplitudes to saturating stimuli of all ligands were similar, although a residual activity of 10–30% of the pre-stimulus level was observed in cells saturated with minor receptor ligands (Figure 1B). The resulting threshold sensitivity S_T, defined as EC_{50}^{-1}, which reflects the lower limit of the concentration range that can be sensed by chemotactic cells, was highest for sugars and only slightly lower for dipeptides and natural amino acids (Figure 1C; Supplementary Table SI).

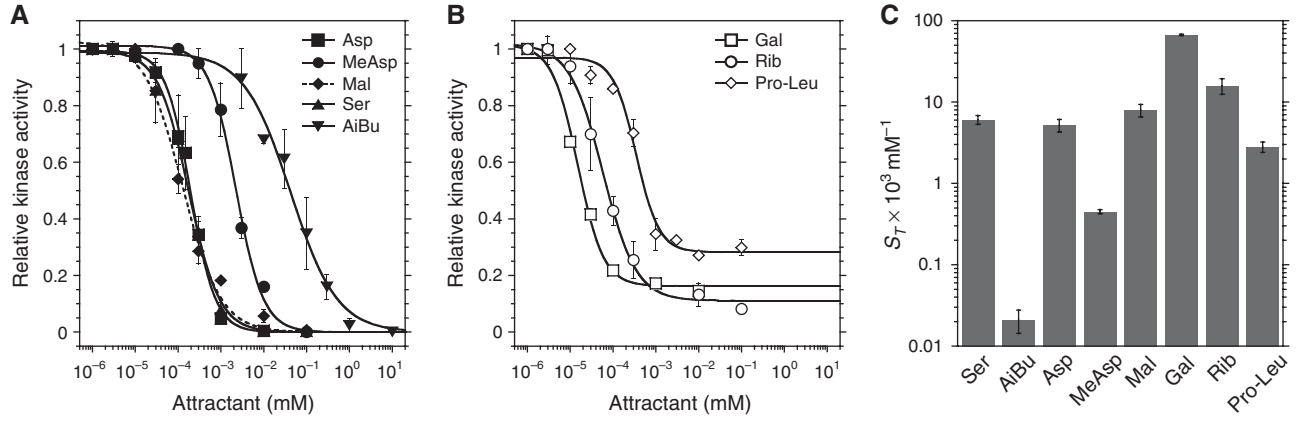

Figure 1 Response of major and minor receptors to attractants. Dose responses of wild-type cells to ligands of major (**A**) and minor receptors (**B**). Cells were stimulated by step-like addition of increasing amounts of attractant. The following abbreviations are used here and throughout: Asp, L-aspartate; MeAsp, α-methyl-DL-aspartate; Ser, L-serine; AiBu, α-aminoisobutyrate; Mal, maltose; Gal, galactose; Rib, ribose; Pro-Leu, proline-leucine dipeptide. Resulting initial changes in kinase activity were measured using a FRET activity reporter (see main text and Materials and methods). After each stimulation, the cells were re-adapted to buffer. The response for each step was normalized to the response of buffer-adapted cells towards a saturating stimulus of 100 μM MeAsp. (**C**) Threshold sensitivity S_T, determined as EC_{50}^{-1} from Hill fits to the dose-response curves of individual experiments. Error bars indicate standard errors.

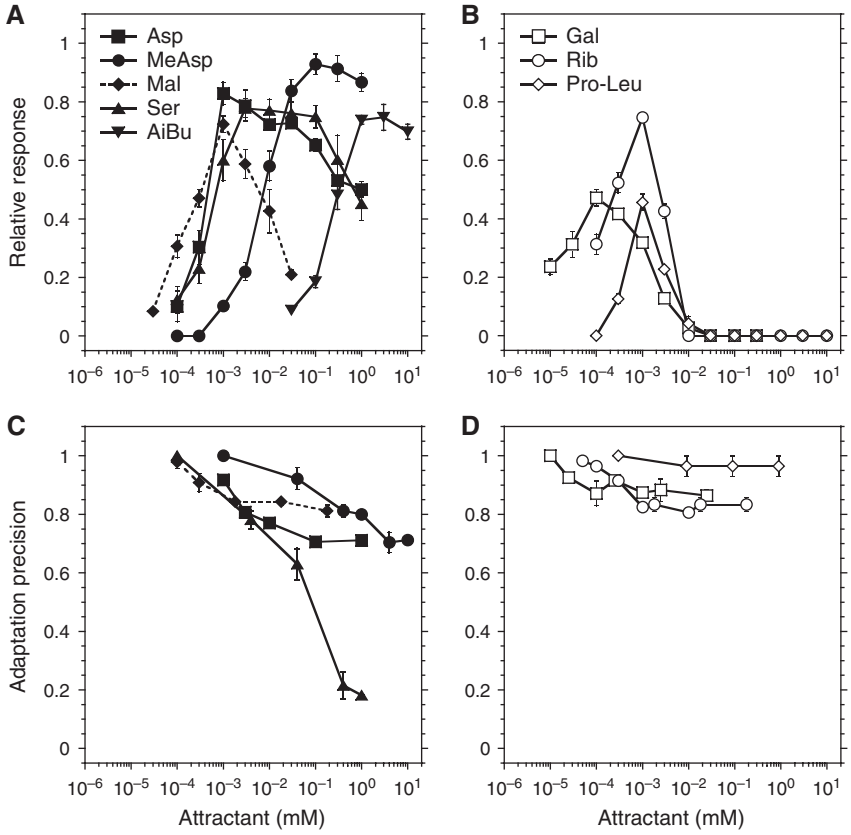

Figure 2 Dynamic range and adaptation precision. Dynamic range (**A**, **B**) and adaptation precision (**C**, **D**) for major (**A**, **C**) and minor (**B**, **D**) receptors. For dynamic range measurements, concentrations were raised in three-fold steps, and the cells were allowed to adapt prior to each subsequent stimulation. The response for each step was calculated relative to the response towards a saturating stimulus (100 μM MeAsp for buffer-adapted cells) and is plotted against the final concentration of ligand. Precision of adaptation was defined as the adapted *FRET* value in the presence of a given concentration of ambient ligand, normalized to the adapted value of *FRET* in buffer. In these experiments, duration of adaptation was limited to 45 min. Error bars indicate standard errors.

To minimize the effect of ligand depletion by cells at low-ligand concentrations, these experiments were performed at the highest flow rate possible in our setup, whereby the content of the entire flow chamber was constantly exchanged nearly every second (see Materials and methods). Although such a high flow rate generally increased measurement errors, it resulted in a significant increase in response amplitudes to the lowest concentrations of some ligands when compared with a five-fold lower flow rate (Supplementary Figure S2), and led to modestly higher estimates of the effective threshold sensitivity (Supplementary Table SI). Such reduction of the response threshold by ligand uptake is consistent with previous observations made in capillary assays (Ordal and Adler, 1974; Hazelbauer, 1975; Zhang *et al*, 1999), and its extent was ligand-dependent as expected from differences in the rates of ligand uptake. Only minor effects were observed for aspartate or galactose, whereas depletion effects for serine or ribose were substantially larger. However, in all cases, the effective reduction in ligand concentration was on the order of EC_{50}, meaning that ligand depletion should not affect the response behaviour at higher ligand concentrations.

Dynamic range of response

The dynamic range over which a sensor can discriminate stimuli of varying strengths is an important property of any sensory system. We determined the dynamic range for a particular ligand by increasing its concentration in approximately three-fold steps (Figure 2A and B; Supplementary Figure S3A and B). In contrast to dose-response measurements, cells in these experiments were allowed to adapt to the current ambient concentration before being stimulated with a next step of increased concentration. Responses to directly binding ligands showed a wide dynamic range and large response amplitudes across this range (Figure 2A). In most of the range, each three-fold increase in aspartate, MeAsp, serine, or AiBu concentration elicited a saturating response, bringing the kinase activity initially close to zero. In contrast, the Tar-mediated response to the indirectly binding ligand maltose was limited to a relatively narrow concentration range, covering only 2–3 orders of magnitude of attractant concentration (Figure 2A), and the dynamic ranges of the responses mediated by indirectly binding ligands of minor receptors were even narrower (Figure 2B). The measured dynamic range may be modestly narrowed for some directly and indirectly binding ligands by their depletion, to the same extent as in the dose-response measurements (Supplementary Table SI; Supplementary Figure S2). However, the effects of depletion are limited to very low ligand concentrations and should neither affect the height at the peaks nor the overall shapes of the dynamic range curves.

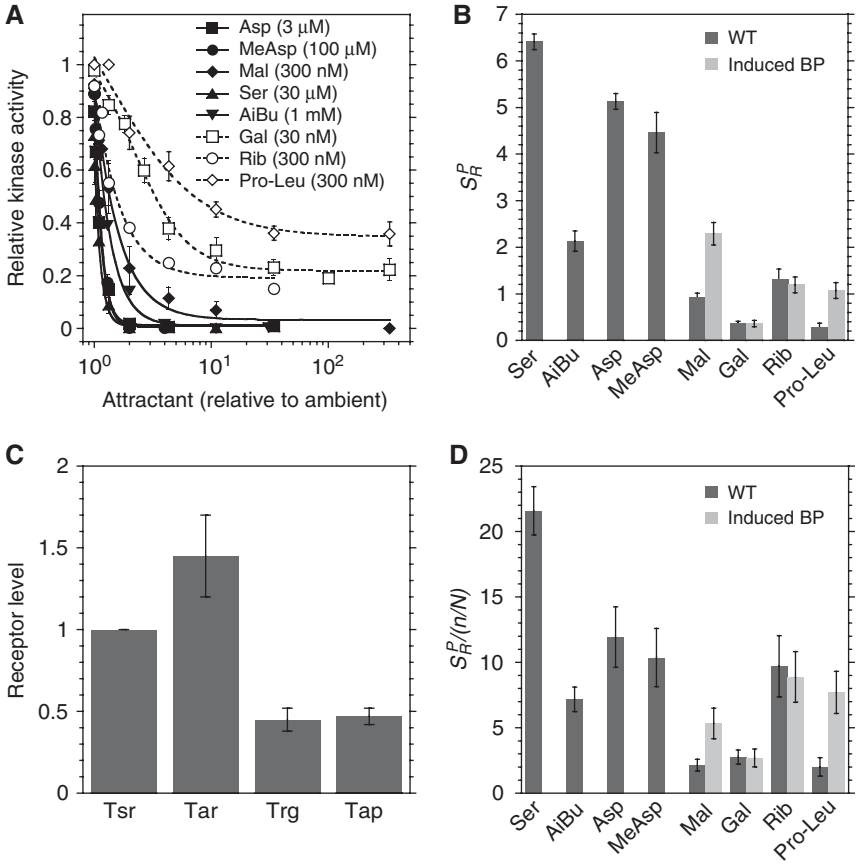

Figure 3 Response sensitivity of major and minor receptors. (**A**) Dose-response curves for cells that were pre-adapted to an ambient concentration of the respective ligand around the peak of the dynamic range (shown in brackets). Kinase activity is plotted as a function of final ligand concentration, normalized to the respective ambient concentration. (**B**) Response sensitivity at the peak of the dynamic range, S_R^P, for WT and otherwise wild-type cells each expressing a plasmid-encoded periplasmic binding protein (BP) at maximum induction of 10 μM salicylate. See text for the definition of S_R^P. (**C**) Native expression levels of receptors in wild-type cells normalized to Tsr, determined by immunoblot as described in Materials and methods and in Supplementary Figure S4. (**D**) S_R^P values from (**B**) normalized to the receptor fraction. Error bars indicate standard errors.

In the high-concentration regime, the dynamic range of the directly binding ligands was apparently limited by the gradually decreasing value of the adapted kinase activity, that is by the imprecision of adaptation (Figure 2A and C; Supplementary Figure S3A and E). The imprecision of adaptation was particularly pronounced for serine, consistent with previous observations (Berg and Brown, 1972). In contrast, adaptation to the indirectly binding ligand maltose (Figure 2C) and minor-receptor ligands (Figure 2D; Supplementary Figure S3B) was relatively precise, indicating that the dynamic range of these ligands was limited by saturation of the sensory system rather than by failure of adaptation, as illustrated in Supplementary Figure S3C–F.

Response sensitivity

Another apparent difference between ligands was in the response amplitude at the peak of the dynamic range, which reflects the response sensitivity S_R to relative changes in concentration of a particular ligand, defined as the ratio between the fractional change in activity ($\Delta A/A$) and the fractional change in ligand concentration ($\Delta L/L$). The value of response sensitivity at the peak of the dynamic range, S_R^P, could in principle be estimated from our dynamic range measurements (Figure 2A and B), but such direct estimation of S_R^P was rather imprecise, and not possible for the directly binding ligands because the three-fold concentration steps were already saturating for these ligands. To determine S_R^P more precisely, dose-response curves were acquired for cells that were pre-adapted to ambient concentrations around the peak of the dynamic range. Plotting these dose-response curves against the relative ligand concentration suggests that indirectly binding ligands are on average less potent in inactivating allosteric receptor teams in wild-type cells (Figure 3A and B). However, this difference was reduced by the overexpression of BPs from salicylate-inducible expression constructs in the wild-type background (Figure 3B).

Quantification of receptor levels

Allosteric models of signal processing by the receptor complexes predict that the response mediated by a particular ligand depends on the number n of specific receptors in a typical signalling team of overall size N. The observed differences in S_R^P and dynamic range might thus be partly due to differences in expression of specific receptors. We therefore quantified the relative cellular levels of all four chemoreceptors by immunoblot analyses, using antibodies raised against signalling domains of Tar and Trg. Because of the high-sequence homology of the signalling domains, these

antibodies recognize all chemoreceptors, but with varying specificity. To calibrate the relative antibody specificity for individual receptors, we compared signal intensities in immunoblots with defined amounts of receptor fusions to YFP, adjusted using both the YFP fluorescence and immunoblotting with GFP-specific antibody that equally well recognizes YFP (see Supplementary Figure S4, Materials and methods, and Supplementary data). The αTar antibody was found to recognize Tar and Tsr with comparable specificity (Tar/$\mathrm{Tsr}_{\alpha\mathrm{Tar}}$: 1.39 ± 0.23), and was therefore used to determine the relative levels of these receptors. The αTrg antibody has similar specificity for minor receptors and Tsr (Trg/$\mathrm{Tsr}_{\alpha\mathrm{Trg}}$: 1.64 ± 0.13; Tap/$\mathrm{Tsr}_{\alpha\mathrm{Trg}}$: 1.23 ± 0.08) and was used for the relative quantification of the minor receptors.

Our results showed that Tap and Trg are less abundant than Tar and Tsr, but in contrast to previous estimates (Li and Hazelbauer, 2004), we only observed a two- to three-fold difference in their levels (Figure 3C; Supplementary Figure S4D). The absolute expression level of Tsr was estimated to be around 6000 copies per cell (Supplementary Figure S5). Comparable receptor ratios were observed for the more conventionally used chemotaxis strain RP437 (Supplementary Figure S4E). It should be noted that the ratio between the levels of major receptors is known to depend on the optical density of the culture (Salman and Libchaber, 2007; Kalinin *et al*, 2010), and we demonstrated a similarly steep dependence for the relative levels of Trg and Tap to Tsr (Supplementary Figure S6). Nevertheless, as the same growth conditions were used to evaluate receptor levels and response parameters in our experiments, we could use the obtained relative receptor amounts to normalize the response sensitivity for respective ligands. Assuming that the relative expression levels reflect the receptor fraction in a signalling team (n/N), we can normalize S_R^P by that fraction to obtain values that are independent of n and thus directly reflect the signalling properties of individual ligands (Figure 3D). Such normalization confirmed that minor and major receptor ligands can signal with similar strengths, although some indirectly binding ligands showed weaker responses even after normalization. Surprisingly, sensitivity of the response to serine was markedly higher than for other directly binding ligands, including the Tsr ligand AiBu. This could not be explained solely by binding properties of serine to Tsr, but was apparently due to a Tsr-independent response to serine in the range of concentrations used to determine S_R^P (Supplementary Figure S7). This Tsr-independent response was also observed in a Tar-only strain (data not shown), indicating that the response may be mediated by Tar, but its exact nature remains to be investigated.

Dependence of response parameters on expression levels of periplasmic BPs and receptors

We observed that the response to indirectly binding ligands strongly depends on expression levels of BPs. Raising levels of BPs specific for galactose (MglB) and Pro-Leu (DppA) through expression from a salicylate-inducible plasmid construct in mutants deleted for the respective endogenous BPs gradually increased response amplitude (Figure 4A) and S_T (Figure 4B) for the corresponding ligands. Consistent with that, an increase in S_T for all indirectly binding ligands except galactose was also observed upon overexpression of the respective BPs in the wild-type background (Supplementary Table SI). Expression of the BPs also affected the values of S_R^P (Figures 3B, 3D, and 4C; Supplementary Figure S8A–C; and Supplementary Table SI), whereby the height of the peak of the dynamic range increased with [BP] and the position of the peak shifted slightly towards lower ligand concentrations, as predicted by our mathematical model of signalling by indirectly binding ligands (see below). The value of S_T (Figure 4B) and the dynamic range (Figure 4C) for galactose in wild-type cells, as well as the results of BP overexpression in WT cells (Supplementary Table SI), confirm that the GBP (or MglB) is fully induced under our growth conditions, whereas BPs for dipeptides, ribose, and maltose are not.

Similarly, increased expression of Tar and Trg resulted in a gradual increase in S_T for MeAsp and galactose, respectively (Figure 4D). Receptor overexpression further led to an expansion of the dynamic range and an increased S_R^P, as illustrated for Trg (Supplementary Figure S8D). The dependence of S_T on the level of receptor expression can be fitted well by assuming simple scaling with the fraction of that particular receptor in the total receptor pool (Figure 4D). Best-fit values for the total receptor level relative to Tsr yield estimates of 3.1 ± 0.8 and 3.6 ± 1.2 for Tar and Trg titrations, respectively, consistent with the estimate obtained by immunoblotting (3.4 ± 0.3; Supplementary Table SI). The similarity of titration curves for Tar and Trg confirms that major and minor receptors behave essentially identically in allosteric complexes.

Mathematical model of minor receptor signalling

The allosteric MWC model for receptors predicts that a tightly coupled team of receptors turns *on* or *off* as a whole, with the activity A, that is the probability of being *on*, determined solely by the free-energy difference between the *on* and *off* states summed over all receptors in the team, $A = [1 + \mathrm{e}^{\sum_r n_r f_r}]^{-1}$, where f_r is the free-energy difference for receptors of type r (with energies expressed in units of the thermal energy k_BT), and n_r is the number of such receptors in the team (Mello and Tu, 2005; Endres and Wingreen, 2006; Keymer *et al*, 2006; Hansen *et al*, 2008). For receptors that directly bind ligand, with [L] as the ligand concentration,

$$f_r = \varepsilon_r + \log \frac{1 + \frac{[L]}{K_r^{off}}}{1 + \frac{[L]}{K_r^{on}}}, \qquad (1)$$

where K_r^{on} and K_r^{off} are the binding constants in the *on* and *off* states for a specific type of receptor r and ε_r is the offset energy in the absence of ligand. For receptors that indirectly bind ligand, with [BP] the BP concentration,

$$f_r = \varepsilon_r + \log \frac{1 + \frac{\tilde{p}_0[\mathrm{BP}]}{\tilde{K}_r^{off}} + \frac{[\mathrm{BP}]}{\tilde{K}_r^{off}} \left(\frac{[L]}{[L]+K_{\mathrm{BP}}} \right)}{1 + \frac{\tilde{p}_0[\mathrm{BP}]}{\tilde{K}_r^{on}} + \frac{[\mathrm{BP}]}{\tilde{K}_r^{on}} \left(\frac{[L]}{[L]+K_{\mathrm{BP}}} \right)}, \qquad (2)$$

where $\tilde{K}_r^{on}$ and $\tilde{K}_r^{off}$ are binding constants of an *on* and *off* receptor to the closed BP, $\tilde{p_0}$ reflects the proportion of closed BP in the absence of ligand, and K_{BP} is a binding constant of BP to ligand (see Supplementary data for full derivations). As precise adaptation returns the total free-energy difference to a fixed value, the response of activity to a change in ligand concentration depends only on the resulting free-energy change. Therefore, experimental dose-response curves

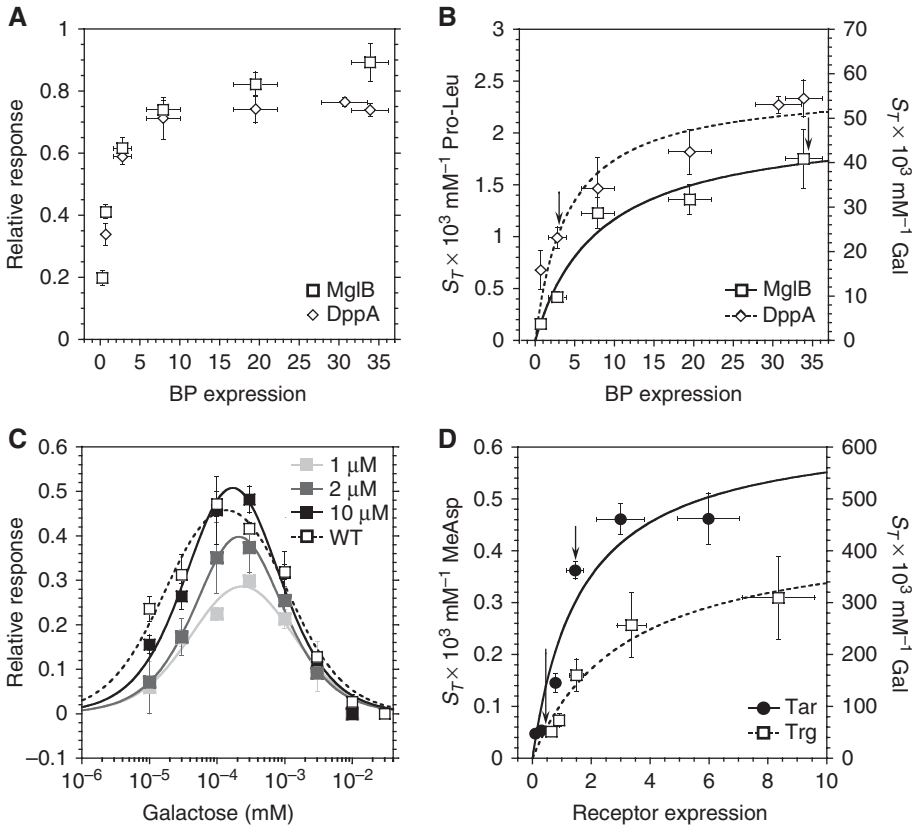

Figure 4 Dependence of chemotactic response on binding protein (BP) and receptor expression. (**A**) Response amplitudes to saturating stimuli of dipeptide Pro-Leu at varying levels of DppA or to galactose at varying levels of MglB. (**B**) Threshold sensitivity S_T of the response to the dipeptide Pro-Leu at varying levels of DppA or to galactose at varying levels of MglB. Arrows mark the native BP expression level estimated from S_T of wild-type cells. (**A**, **B**) Dipeptide BP DppA was expressed at different levels of salicylate induction in a Δ*dppA* strain, and the galactose BP MglB was expressed in a Δ*mglB* strain. Expression of BPs was assumed to be proportional to the expression of yellow fluorescent protein (YFP) from the same promoter, measured by FACS and used for the *X* axis. The data were fitted using the function $S_T = S_T^{\max}[\mathrm{BP}]/(C + [\mathrm{BP}])$, where C is a constant (see equation (3)). (**C**) Dynamic range of the response to galactose at varying expression of MglB. The three highest expression levels in the Δ*mglB* background from (**A**) are shown, with darker grey levels corresponding to higher expression. The wild-type dynamic range is shown for comparison. Data were fitted using the function $S_R = C_1C_2[\mathrm{L}]/((C_2 + [\mathrm{L}])([\mathrm{L}] + C_3))$, where C_1, C_2, and C_3 are constants (see equation S18 in Supplementary data). (**D**) Threshold sensitivity of the response to MeAsp at varying levels of Tar or to galactose at varying levels of Trg. Tar was expressed at different levels of salicylate induction in a Δ*tar* strain; Trg was expressed in the wild-type strain. Receptor expression levels were determined as in Figure 3C and normalized to the native expression of Tsr. Data were fitted using the function $S_T = S_T^{\max}[\mathrm{R}]/([\mathrm{R}] + C)$, where C is a constant describing the expression level of all other receptors. Response amplitudes were nearly saturating at all measured expression levels. Arrows mark the native expression levels of Trg and Tar. Error bars indicate standard errors.

should collapse when plotted as a function of this free-energy change. For different receptor types, the free-energy change must be weighted by the receptor proportion to yield an average, $\langle \delta f \rangle = (n_r/N)\delta f_r$, where n_r is the number of receptors of type r in a team of N receptors. Using the receptor ratios from Figure 3C, we calculated the change in free energy upon addition of more ligand to cells adapted to ambient ligand concentration, and from the best-data collapse obtained the binding parameters given in Supplementary data. The results for WT cells (Figure 5) prove the ability of the model to account for responses of both kinds of ligands. From the free-energy expressions, both the threshold sensitivity S_T and the response sensitivity S_R can be calculated. For both direct and indirect ligand binding, S_T and S_R are proportional to the number n_r of ligand-specific receptors in a signalling team, as observed experimentally (Figure 4D). The indirect ligand-binding model predicts that significant *on* receptor binding to BP would cause a decrease in both S_T and S_R at high [BP]. However, this decrease of sensitivity at high [BP] is not observed (Figure 4A and B). Instead, both S_T and S_R saturate at the highest levels of [BP] measured. From the model, we conclude that S_T and S_R saturate with increasing [BP] as *off* receptors begin to significantly bind BP in the absence of ligand. In the regime of parameters inferred from the data collapse ($\tilde{K}_r^{off} \ll [\mathrm{BP}] \ll \tilde{K}_r^{on}$, and $\tilde{p}_0 \ll 1$), S_T and S_R^p have the simple forms,

$$S_T \approx S_T^{\max}[\mathrm{BP}]/(\tilde{K}_r^{off}/\tilde{p}_0 + [\mathrm{BP}]), \tag{3}$$

$$S_R^p \approx n_r(1 - A_0)\left[1 - 2\sqrt{\tilde{K}_r^{off}/[\mathrm{BP}] + \tilde{p}_0}\right]. \tag{4}$$

In the same experimental regime, the peak in response sensitivity also shifts with [BP] as

$$[L^p] \approx K_{\mathrm{BP}}\sqrt{\tilde{K}_r^{off}/[\mathrm{BP}] + \tilde{p}_0}. \tag{5}$$

From the estimated parameters, the response sensitivity S_R^p for receptors that indirectly bind ligand is much lower than the maximum possible value of n_r $(1-A_0)$. For receptors that bind ligand directly, as long as adaptation remains precise or

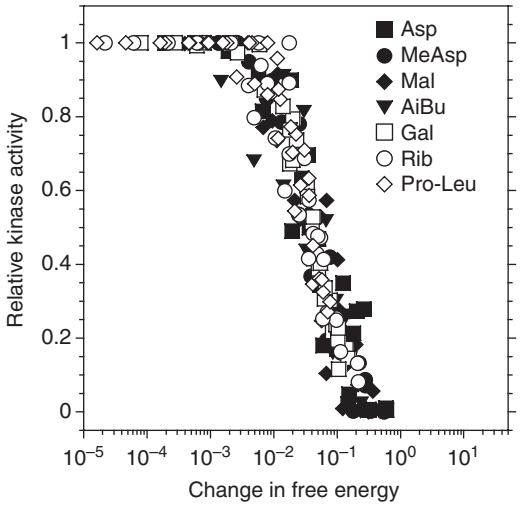

Figure 5 Collapse of receptor activity when plotted as a function of free-energy change. Results are shown for wild-type cells responding to indicated ligands. Binding parameters were obtained through the collapse of normalized dose-response and dynamic-range curves of both wild-type cells and cells at different BP induction levels. The free-energy model for BP-binding ligands (Approximation 1) and binding parameters are described in Supplementary data. The observed ratios Tar: Tsr: Tap: Trg of 1.5:1:0.5:0.5 were used for the collapse.

nearly so, loss of response sensitivity is due to binding of ligand by *on* receptors, but for BP-binding receptors, in addition to binding of closed BP by *on* receptors, additional losses in sensitivity occur because: (i) receptors bind to open BPs, (ii) there are some closed BPs even in the absence of ligand, and (iii) the BP concentration may be non-optimal. These additional factors help explain the lower response sensitivities observed for receptors that bind BPs compared with receptors that bind ligand directly (Figure 3A and B). Our mathematical model and the obtained data collapse thus not only allow us to evaluate response parameters for the indirectly binding ligands, but also yield a better understanding of the advantages and disadvantages of the two distinct modes of ligand binding.

Signal integration

In its natural environment, *E. coli* typically encounters complex mixtures of chemoeffectors, but signal integration by cells stimulated with combinations of different ligands has not been well studied until now. To investigate signal integration, we first compared responses to simultaneous excitation with two different ligands with responses elicited by these ligands individually. As illustrated for the example of galactose and MeAsp (Figure 6A), we first determined dose-response curves for each attractant individually, and then stimulated the same cells with a mixture of approximately equipotent concentrations of the two ligands, for example 10 nM galactose and 1 μM MeAsp. For sub-saturating stimuli, such stimulation produced response amplitudes that were approximately twice the size of the response amplitudes elicited by corresponding concentrations of galactose or MeAsp individually, indicating simple summation of the chemotactic responses. Further computational analysis confirmed that this summation could be accounted for by additivity of changes in free energy because of binding of galactose and MeAsp to the mixed signalling teams (Figure 6A, dashed line). Consistent with this summation of signal, when cells were pre-adapted to 8 μM MeAsp and then stimulated with different concentrations of galactose while removing MeAsp, the sign of the response depended solely on the relative strengths of both stimuli (Figure 6B). Nearly no response was observed for simultaneous addition of one and removal of the other ligand at approximately equipotent concentrations, 50 nM galactose and 8 μM MeAsp in this example. Similar results were obtained for other ligands (data not shown). In all cases, signal integration did not depend on the type of ligand binding.

We further addressed the question of how adaptation to a saturating concentration of one ligand affects responses to other ligands. For two ligands that are sensed by different receptors, the response to a second ligand was nearly unaffected by the presence of the first (Figure 6C and D; Table I), although a slight increase in the threshold sensitivity was observed in most cases. Such an increase may be explained by the imprecise adaptation to the ambient ligand, as lower adapted activity of the receptor team A_0 is expected to increase S_T (see equation 30 in Supplementary data). The increase in sensitivity may also be due in part to an increased receptor team size, following the increase in the receptor methylation level upon adaptation (Endres *et al*, 2008). Interestingly, no significant interference with the threshold sensitivity $S_T$could be observed between MeAsp and maltose, the directly and indirectly binding ligands of Tar (Figure 6D; Table I), which confirms previous observations that these ligands can be sensed independently even though they share a receptor (Mowbray and Koshland, 1987; Gardina *et al*, 1998). In contrast, the indirectly binding ligands sensed by Trg clearly affected each other's responses, with sensitivity and response amplitude towards galactose being markedly reduced upon adaptation to ribose, and *vice versa* (Figure 6C; Table I). This clearly indicated competition of the ligand-loaded periplasmic BPs for Trg, consistent with previous observations (Adler *et al*, 1973; Strange and Koshland, 1976). The observed asymmetry in the mutual effects of galactose and ribose on each other's responses (Table I) may indicate a higher affinity of the ligand-loaded ribose BP to Trg (Yaghmai and Hazelbauer, 1993). However, in none of the cases was the response completely blocked by the presence of another ligand, suggesting that even at saturating levels of stimulation receptors are not fully occupied by either BP at our wild-type BP concentrations.

Even stronger competition was observed between galactose and glucose, which signal to Trg through the same BP (GBP). As the sensitivity of response of buffer-adapted cells to either ligand is essentially the same (Table I), the adaptation to a saturating concentration of glucose completely inhibited the response to galactose, consistent with the competitive binding of both ligands to GBP (Anraku, 1968; Adler *et al*, 1973). In contrast, a saturating amount of galactose only shifted the response to glucose towards higher concentrations, where the response to glucose is most likely mediated by the phosphotransferase system (PTS; Adler *et al*, 1973; Adler and Epstein, 1974). Response to glucose with comparable EC_{50} (0.18 ± 0.03 μM) and response amplitude was also observed in the *trg* strain. The PTS thus apparently provides a backup system that allows cells to sense a high enough concentration of glucose, a preferred carbon source, even when the periplasmic BP is saturated by another ligand.

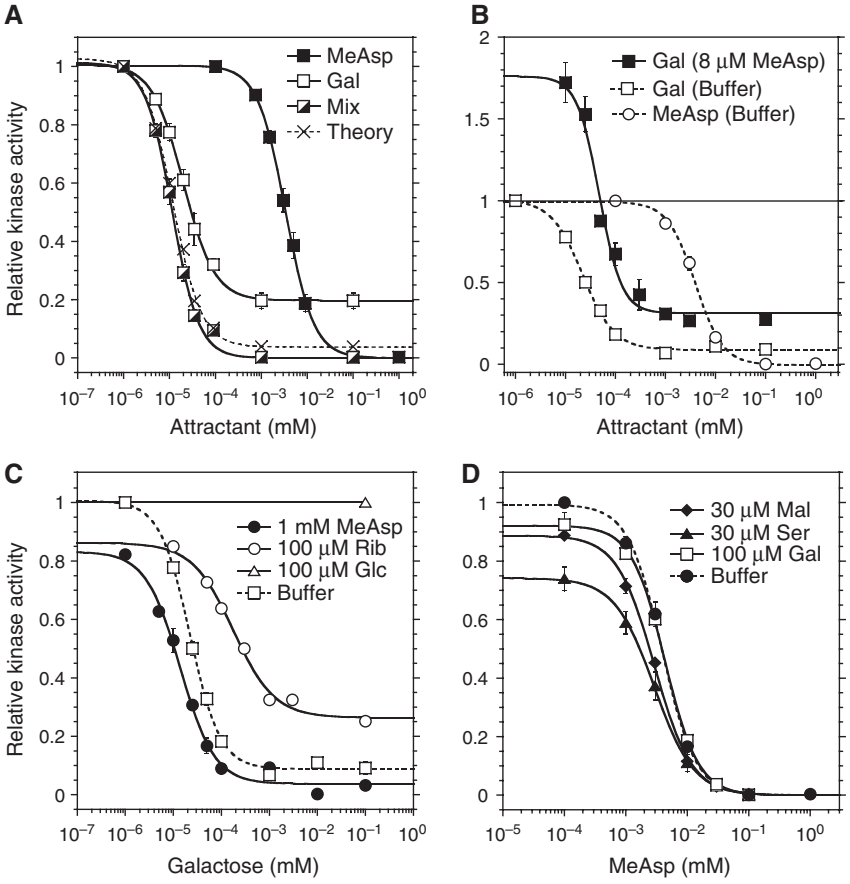

Figure 6 Responses to simultaneous stimulation with multiple ligands. (**A**, **B**) Signal integration. (**A**) Integration of stimuli of the same sign. Dose responses were acquired for buffer-adapted cells to MeAsp and galactose separately, and then to simultaneous addition of the both MeAsp and galactose at concentrations found to be equipotent from the single-attractant dose-response curves. Responses to the galactose–MeAsp mixture are plotted against galactose concentration. Crosses and dashed line indicate model prediction for the response to the galactose–MeAsp mixture assuming summation of the free energies of ligand binding to the mixed signalling teams. Lines here and throughout are Hill fits to the data. (**B**) Integration of stimuli of opposing signs. Cells were pre-adapted to 8 μM MeAsp and then stimulated by indicated concentrations of galactose in the buffer. The solid horizontal line indicates the adapted kinase activity at 8 μM MeAsp. No response was observed upon stimulation with the galactose concentration equipotent to 8 μM MeAsp. Below this concentration, the response was negative (increase in kinase activity), whereas above this concentration, the response was positive (decrease in kinase activity). Responses of buffer-adapted cells to galactose and to MeAsp are shown for a reference. A slight difference in the amplitude of the saturated response for galactose in (**A**, **B**) is presumably due to variance in the native expression level of GBP. (**C**, **D**) Effects of adaptation to other ligands on dose responses. (**C**) Responses to galactose of cells adapted to buffer, 1 mM MeAsp, 100 μM ribose, or 100 μM glucose. (**D**) Responses to MeAsp of cells adapted to buffer, 100 μM galactose, 30 μM serine, or 30 μM maltose.

Discussion

In this work, we have quantitatively compared signalling mediated by ligands for all four *E. coli* chemoreceptors. In contrast to the common classification in chemotactic sensing, which primarily distinguishes between major (high abundance) and minor (low abundance) receptors, our data suggest that minor receptors are significantly more abundant than previously believed, constituting more than a quarter of the total receptor pool, and that the main distinction thus must be made between directly and indirectly binding ligands. Our analysis of response features that are expected to be important for cells to navigate in chemical gradients—threshold sensitivity S_T, dynamic range, and response sensitivity to fractional changes in ligand concentration S_R—showed that responses mediated by these two types of ligands are distinctly different.

The discrepancy of our results with the previously reported values of receptor abundance (Hazelbauer *et al*, 1981; Li and Hazelbauer, 2004) can be partly attributed to differences in the culture growth conditions, as the relative levels of receptors strongly depend on the optical density of the culture (Salman and Libchaber, 2007; Kalinin *et al*, 2010; Supplementary Figure S6). Moreover, the total relative levels of minor receptors, including those of Tap, were previously estimated only indirectly (Hazelbauer *et al*, 1981; Li and Hazelbauer, 2004 and references therein), which apparently led to a significant underestimation. Most importantly, our study uniquely enabled a direct comparison between the levels and response of individual receptors, because both were measured under identical growth conditions.

Similarity of the normalized response sensitivity values, S_R^p, for different ligands suggest that all receptors in an allosteric signalling team can mediate responses of comparable magnitude and sensitivity, irrespective of their type and the mode of ligand binding. This is consistent with the existing mathematical description of chemosensory complexes, which predicts that the response sensitivity

Table I Effects of adaptation to a saturating level of an ambient ligand on responses to other ligands

Condition	Attractant	Ambient	EC_{50} (without ambient) (μM)[a,b]	EC_{50} (with ambient) (μM)
Directly binding ligands sensed by different receptors	MeAsp	30 μM Ser	4.0 ± 0.4	3.0 ± 0.2
	Ser	1 mM MeAsp	0.47 ± 0.06	0.40 ± 0.03
Indirectly and directly binding ligand sensed by different receptors	Gal	1 mM MeAsp 30 μM Ser	0.023 ± 0.002	0.014 ± 0.002
	Gal	1 mM MeAsp		0.015 ± 0.002
	MeAsp	100 μM Gal	4.0 ± 0.4	4.4 ± 0.15
Indirectly and directly binding ligand sensed by the same receptor	MeAsp	30 μM Mal	4.0 ± 0.4	3.0 ± 0.2
	Mal	1 mM MeAsp	0.18 ± 0.01	0.23 ± 0.01
Indirectly binding ligands recognized by the same receptor via different BPs	Gal	100 μM Rib	0.023 ± 0.002	0.18 ± 0.03
	Rib	100 μM Gal	0.16 ± 0.02	0.34 ± 0.02
Indirectly binding ligands recognized via the same BP	Gal	100 μM Glc	0.023 ± 0.002	No response
	Glc	100 μM Gal	0.026 ± 0.004	0.19 ± 0.02

[a]Experiments were performed at a flow rate of 500 μl/min.
[b]Error bars indicate standard errors.

primarily depends on the fraction of ligand-specific receptors in a signalling team, and further validates our estimates of the relative expression levels of individual receptors. In addition, response sensitivity for both modes of binding is influenced by the ratio of binding affinities of the ligand towards *on* and *off* states of receptors (equation S16 in Supplementary data), explaining the residual variation of sensitivity towards directly binding ligands after normalization for the level of receptor expression. An exception was the response towards serine, which showed distinctly higher sensitivity, apparently because of a second, Tsr independent, sensory system.

Stimulation with different ligand combinations demonstrated that responses mediated by different receptors in the sub-saturating stimulus range are additive. This confirms predictions of allosteric models of signalling, which suggest that the sign and the magnitude of the response are determined by the net change in the stimulus strength, that is by the free-energy change due to ligand binding. Receptors in clusters thus integrate signals using 'majority voting' to navigate in mixed gradients, consistent with early analyses of chemotaxis using capillary assays (Adler and Tso, 1974). Moreover, we observed that the response to a given ligand is not substantially affected by the adaptation to saturating levels of other ligands, which apparently allows the chemotaxis system to maintain high sensitivity at high levels of background stimulation. An exception is signalling by ligands that compete for the same receptor or for the same BP, in which case the response is reduced or even entirely abolished by high levels of competing ligands.

How can cells regulate their ligand preferences? Our experiments confirmed that the response sensitivity for both modes of binding grows in proportion to the receptor fraction in a signalling team. For the indirectly binding ligands, however, the response further depends on the binding characteristics and availability of the associated periplasmic BP, and a response with maximal sensitivity is only observed when BPs are expressed in excess of receptors, which is consistent with previous studies (Manson *et al*, 1985). The effects of BP expression on response are unlikely to be related to the depletion of free ligand-bound BPs from the periplasm by their association with membrane transporters, because the expression levels of BPs are believed to be much higher than the levels of their transporters (Manson *et al*, 1985; Higgins *et al*, 1990). Rather, our analysis suggests that the uninduced expression of most BPs under our growth conditions is not sufficient to saturate receptors upon ligand binding. Furthermore, we observed that, even when BPs are overexpressed, the response sensitivity for some indirectly binding ligands can be significantly lower. This is illustrated by the comparison of two Trg ligands, galactose and ribose: whereas S_R^P for ribose is essentially the same as for the directly binding ligands, the value for galactose is nearly three-fold lower. Our mathematical model of signalling by the indirectly binding ligands suggests that such loss of sensitivity can be explained by the residual BP binding to receptor even in the absence of ligand, as this would reduce the signalling effect of ligand binding.

The dependence of response towards a particular ligand on the relative expression levels of receptors and of BPs means that sensitivity can be dynamically controlled by cells, dependent on growth or environmental conditions. From this perspective, indirect ligand binding provides an additional flexibility in regulation. This flexibility comes, however, at the cost of a narrower dynamic range. Although the extension of the dynamic range towards low concentrations is likely to have been modestly underestimated for some ligands because of their depletion, the dynamic range of the indirectly binding ligands is clearly much narrower than that of the directly binding ligands. For direct ligand binding, the major extension of the dynamic range is achieved by the adaptation system (Supplementary Figure S3C and E). Adaptive receptor methylation maintains the sensitivity of the system at high-ligand concentrations and returns the kinase activity to a preset level by means of effectively tuning the ligand affinity of receptors between K_r^{off} and K_r^{on} (Endres and Wingreen, 2006; Mello and Tu, 2007; Hansen *et al*, 2008). Thus, the response range for major receptors extends until either (i) receptors become fully methylated and can no longer adapt to added ligand, or (ii) receptors become fully saturated with ligand (i.e. $[L] > K_r^{on}$) and can no longer respond to added ligand. Consistent with this picture, the dynamic range for the directly binding ligands spans 4–5 orders of magnitude (Mesibov and Adler, 1972; Sourjik and Berg, 2002). Our data suggest that for serine, the dynamic range is indeed limited by the range of receptor adaptation

(case i). In contrast, the dynamic range for aspartate appears to be restricted instead by receptor saturation (case ii), given the estimated value for K_r^{on} of 20 μM of Tar receptors for aspartate and the observed relatively precise adaptation up to 1 mM aspartate.

In contrast, the dynamic range for indirect binding cannot be extended by adaptation, because the range is limited by the occupancy of the BP, and the affinity of the latter for its ligand cannot be adjusted by the adaptation system working on the receptor (Supplementary Figure S3D and F). As a result, cells respond to galactose, ribose, dipeptides, or maltose over only about two orders of magnitude of ligand concentration, consistent with the results of previous capillary assays (Mesibov *et al*, 1973). As a consequence, adaptation to saturating concentrations of indirectly binding ligands results in much smaller changes in receptor methylation than adaptation to directly binding ligands (Supplementary Figure S9).

Given the advantages and disadvantages of the two modes of ligand sensing, what could have led to their evolutionary fixation? For indirectly binding ligands, it can be speculated that coupling of the ABC transport and chemotaxis systems allows better coordination of the rate of ligand-specific nutrient uptake and the chemotactic response. This prevents cell accumulation at excessively high concentrations of attractants and allows a concerted regulation of chemotaxis and transport according to environmental conditions. The expression of periplasmic BPs is typically inducible (Koman *et al*, 1979), so that cells can simultaneously upregulate both uptake and chemotaxis in the presence of the respective ligand. In contrast to response regulation through the level of receptor expression, such BP-dependent regulation allows cells to specifically increase chemotaxis towards one particular ligand without upregulating responses to all other ligands sensed by the same receptor. Moreover, cells would chemotactically follow gradients of the indirectly binding ligand only as long as the uptake system remained unsaturated, and moving up the gradient increased the efficiency of nutrient uptake. At concentrations above transporter saturation, cells will be indifferent to the gradient of that ligand and can instead follow gradients of other attractants. Taxis to carbohydrates such as glucose is further connected to their uptake through the PTS transporters in a receptor-independent manner (Postma *et al*, 1993), which allows cells to selectively extend the dynamic range of the chemotaxis system, again in a tight coupling with the dynamic range of the uptake. Taken together, the indirect sensing of sugars and dipeptides appears to present an evolutionarily optimal strategy to maximize the overall nutrient uptake by specific systems.

This contrasts with the direct sensing of amino acids, which allows cells to follow gradients over a much larger span of concentrations. The physiological reason for this difference remains unclear. In contrast to sugars, the uptake of amino acids such as serine and aspartate in *E. coli* is primarily performed by multiple symporters (Schellenberg and Furlong, 1977; McFall and Newman, 1996; Kim *et al*, 2002), which are not known to mediate any chemotactic responses. The broad dynamic range for these amino acids may therefore enable cells to accumulate at concentrations corresponding to the functional range of symporters without a direct coupling to transport. In addition, the broader dynamic range may be required for the nutrition-unrelated function of chemotaxis towards amino acids, such as signal exchange between bacteria (Budrene and Berg, 1991; Park *et al*, 2003).

Materials and methods

Attractants

L-aspartic acid (>99% purity), α-methyl-DL-aspartic acid (MeAsp), L-serine, 2-aminoisobutyric acid (98% purity), D-(+)-maltose monohydrate (min. 99% purity), D-(+)-galactose (min. 99% purity), D-(+)-glucose, D-(−)-ribose (min. 99% purity), and Pro-Leu were purchased from Sigma. At this purity grade, maltose and galactose are declared to contain <0.3 and <0.1% glucose, respectively. This glucose contamination may lead to an unspecific Trg-mediated response at around 1 mM of these ligands, which set the limits of the concentration range of maltose and galactose used in this study.

Strains and plasmids

All strains and respective genotypes, plasmids and primers used in this study are listed in Supplementary Table SII. SN1 and VS275 were generated by the pAMPts homologous recombination system of allele exchange (Sourjik and Berg, 2000). SN11 was made by P1 transduction with donor VS139 and recipient SN1.

SN27, SN28, and SN31 were made by P1 transduction using respective donor strains from the Keio collection (Baba *et al*, 2006) and SN1 as recipient. The λ-*Red* system (Datsenko and Wanner, 2000) was used to generate both SN25 and SN23. Here, the Kan^R cassette was amplified from Keio strain JW1875 using primers Vic113 and Vic146 and transformed into recipient strains SN1 and VS275 expressing the *Red*-System from the helper plasmid pKD46 by electroporation. After selecting strains on kanamycin (50 μg/ml), the resistance cassette in all strains was flipped out using the curable temperature-sensitive plasmid pCP20 that encodes FLP recombinase.

Preparation of cells

E. coli K-12 strain LJ110 Δ(*cheY cheZ*) and its derivatives were used for all FRET measurements. Cells were grown in tryptone broth supplemented with antibiotics (100 μg/ml ampicillin; 34 μg/ml chloramphenicol) depending on the plasmids present. IPTG was added to a final concentration of 50 μM to induce expression of CheY-YFP and CheZ-CFP from pVS88 (pTrc99a; Amp^R; Sourjik and Berg, 2004). BP and receptor expression from pKG110 derivatives was induced by salicylate in a range of 0–10 μM as indicated. After growth to OD_{600} of 0.45 at 34°C and 275 r.p.m., cells were harvested by centrifugation (10 min at 5000 *g*) and resuspended in the original culture volume of tethering buffer (10 mM KPO_4, 0.1 mM EDTA, 1 μM methionine, 10 mM lactic acid, 67 mM NaCl, pH 7). Protein expression was shut down for at least 30 min at 8°C, before cells were attached to a polylysine-coated coverslip and placed into a flow chamber of 50 μl volume (Berg and Block, 1984; Sourjik *et al*, 2007). The chamber was kept under constant flow of tethering buffer (300 μl/min for dynamic range and adaptation measurements, 500 μl/min for sensitivity measurements, and 2500 or 500 μl/min for dose-response measurements) by a syringe pump (Harvard Apparatus 22) that was stopped briefly to add and remove attractants.

Data acquisition and analysis

Measurements were done as described before (Sourjik and Berg, 2002) on a Zeiss Axio Imager.Z1 microscope equipped with a 40x/0.75 EC Plan-Neofluar objective and controlled by Axiovision software. CFP fluorescence of a dense monolayer was excited at 436/20 nm through a 455 nm dichroic mirror by a 75 W Xenon lamp attenuated 500-fold with neutral density filters. CFP and YFP emissions were detected through 480/40 nm band pass and 520 nm long-pass emission filters, respectively, and signals were collected with an integration time of 1 s by Peltier-cooled photon counters (Hamamatsu) equipped with a PCI-6034 counting board connected to a computer with custom written LabView7 software (both from National Instruments). FRET values were calculated as described previously (Sourjik and Berg, 2002; Sourjik *et al*, 2007; see Supplementary methods for details).

Receptor quantification

Receptor quantification was performed using immunoblot and FACS analyses as described in Supplementary data and in Supplementary Figures S4 and S5. For YFP quantification using FACScan (Becton Dickinson), cells were prepared as for FRET and diluted 1:20. For immunoblots, cells were harvested by centrifugation and resuspended in 1 × Laemmli buffer to give the same YFP concentration, determined by the FACS value, in all samples. Samples were boiled and separated by 10% SDS–PAGE, with several consecutive dilutions of each sample being applied to each gel (Supplementary Figure S4). Proteins were then transferred to a 0.2-μm pore-size Hybond ECL nitrocellulose membrane using tank blotting. Receptor detection was performed using primary polyclonal αTrg (kindly provided by G Hazelbauer) or αTar antibody at 1:5000 dilution and IRDye® 800 conjugated secondary antibody (Rockland) at 1:10 000 dilution. Membranes were scanned with an Odyssey® Imager (LI-COR) and protein bands were quantified using ImageJ software (http://rsbweb.nih.gov/ij). The background signal from empty areas of the membrane was subtracted. Only bands in the linear intensity range were used for subsequent analyses. Specificity of αTrg and αTar antibodies for individual receptors was determined by using YFP fusions to receptors as a reference. To check the consistency of YFP loading in the reference samples, control immunoblotting was performed using αGFP monoclonal antibody (JL-8; Clontech) and IRDye 700 conjugated secondary antibody (Rockland).

Estimation of relative BP expression

Expression of BPs was assumed to be proportional to the expression of YFP controlled by the same promoter (p*nahG*), determined by the FACScan analysis. For FACS, cells expressing eYFP from pVS118 and carrying an empty pTrc99a vector were induced over a range of 0–10 μM salicylate, and grown and prepared as for FRET experiments.

Supplementary data

Supplementary data are available at *The EMBO Journal* Online (http://www.embojournal.org).

Acknowledgements

We thank GL Hazelbauer for the gift of αTrg antibody. This work was supported by grants RGP66/2005 from the Human Frontier Science Program, SO 421/7-1 and SO 421/3-3 from the Deutsche Forschungsgemeinschaft and GM082938 from the National Institutes of Health. VS and NSW acknowledge the hospitality of the Aspen Center for Physics.

Author contributions: VS, SN, and NSW designed the research; SN performed the experimental research; CH and NSW performed the mathematical modelling; VS, SN, CH, and NSW wrote the paper.

Conflict of interest

The authors declare that they have no conflict of interest.

References

Adler J, Epstein W (1974) Phosphotransferase-system enzymes as chemoreceptors for certain sugars in *Escherichia coli* chemotaxis. *Proc Natl Acad Sci USA* **71:** 2895–2899

Adler J, Hazelbauer GL, Dahl MM (1973) Chemotaxis toward sugars in *Escherichia coli*. *J Bacteriol* **115:** 824–847

Adler J, Tso WW (1974) 'Decision'-making in bacteria: chemotactic response of Escherichia coli to conflicting stimuli. *Science* **184:** 1292–1294

Ames P, Studdert CA, Reiser RH, Parkinson JS (2002) Collaborative signalling by mixed chemoreceptor teams in *Escherichia coli*. *Proc Natl Acad Sci USA* **99:** 7060–7065

Anraku Y (1968) Transport of sugars and amino acids in bacteria. I. Purification and specificity of the galactose- and leucine-binding proteins. *J Biol Chem* **243:** 3116–3122

Baba T, Ara T, Hasegawa M, Takai Y, Okumura Y, Baba M, Datsenko KA, Tomita M, Wanner BL, Mori H (2006) Construction of *Escherichia coli* K-12 in-frame, single-gene knockout mutants: the Keio collection. *Mol Syst Biol* **2:** 2006.0008

Berg HC, Block SM (1984) A miniature flow cell designed for rapid exchange of media under high-power microscope objectives. *J Gen Microbiol* **130:** 2915–2920

Berg HC, Brown DA (1972) Chemotaxis in *Escherichia coli* analysed by three-dimensional tracking. *Nature* **239:** 500–504

Berg HC, Purcell EM (1977) Physics of chemoreception. *Biophys J* **20:** 193–219

Bialek W, Setayeshgar S (2005) Physical limits to biochemical signaling. *Proc Natl Acad Sci USA* **102:** 10040–10045

Borkovich KA, Alex LA, Simon MI (1992) Attenuation of sensory receptor signalling by covalent modification. *Proc Natl Acad Sci USA* **89:** 6756–6760

Bray D, Levin MD, Morton-Firth CJ (1998) Receptor clustering as a cellular mechanism to control sensitivity. *Nature* **393:** 85–88

Budrene EO, Berg HC (1991) Complex patterns formed by motile cells of *Escherichia coli*. *Nature* **349:** 630–633

Datsenko KA, Wanner BL (2000) One-step inactivation of chromosomal genes in *Escherichia coli* K-12 using PCR products. *Proc Natl Acad Sci USA* **97:** 6640–6645

Duke TA, Le Novere N, Bray D (2001) Conformational spread in a ring of proteins: a stochastic approach to allostery. *J Mol Biol* **308:** 541–553

Endres RG, Oleksiuk O, Hansen CH, Meir Y, Sourjik V, Wingreen NS (2008) Variable sizes of Escherichia coli chemoreceptor signaling teams. *Mol Syst Biol* **4:** 211

Endres RG, Wingreen NS (2006) Precise adaptation in bacterial chemotaxis through 'assistance neighborhoods'. *Proc Natl Acad Sci USA* **103:** 13040–13044

Gardina PJ, Bormans AF, Manson MD (1998) A mechanism for simultaneous sensing of aspartate and maltose by the Tar chemoreceptor of *Escherichia coli*. *Mol Microbiol* **29:** 1147–1154

Gegner JA, Graham DR, Roth AF, Dahlquist FW (1992) Assembly of an MCP receptor, CheW, and kinase CheA complex in the bacterial chemotaxis signal transduction pathway. *Cell* **70:** 975–982

Gestwicki JE, Kiessling LL (2002) Inter-receptor communication through arrays of bacterial chemoreceptors. *Nature* **415:** 81–84

Hansen CH, Endres RG, Wingreen NS (2008) Chemotaxis in *Escherichia coli*: a molecular model for robust precise adaptation. *PLoS Comput Biol* **4:** e1

Hazelbauer GL (1975) Maltose chemoreceptor of *Escherichia coli*. *J Bacteriol* **122:** 206–214

Hazelbauer GL, Engstrom P, Harayama S (1981) Methyl-accepting chemotaxis protein III and transducer gene trg. *J Bacteriol* **145:** 43–49

Hazelbauer GL, Mesibov RE, Adler J (1969) *Escherichia coli* mutants defective in chemotaxis toward specific chemicals. *Proc Natl Acad Sci USA* **64:** 1300–1307

Higgins CF, Gallagher MP, Hyde SC, Mimmack ML, Pearce SR (1990) Periplasmic binding protein-dependent transport systems: the membrane-associated components. *Philos Trans R Soc Lond B Biol Sci* **326:** 353–364

Kalinin Y, Neumann S, Sourjik V, Wu M (2010) Responses of *Escherichia coli* bacteria to two opposing chemoattractant gradients depend on the chemoreceptor ratio. *J Bacteriol* **192:** 1796–1800

Keymer JE, Endres RG, Skoge M, Meir Y, Wingreen NS (2006) Chemosensing in *Escherichia coli*: two regimes of two-state receptors. *Proc Natl Acad Sci USA* **103:** 1786–1791

Kim YM, Ogawa W, Tamai E, Kuroda T, Mizushima T, Tsuchiya T (2002) Purification, reconstitution, and characterization of Na(+)/serine symporter, SstT, of *Escherichia coli*. *J Biochem* **132:** 71–76

Koman A, Harayama S, Hazelbauer GL (1979) Relation of chemotactic response to the amount of receptor: evidence for different efficiencies of signal transduction. *J Bacteriol* **138:** 739–747

Lai RZ, Manson JM, Bormans AF, Draheim RR, Nguyen NT, Manson MD (2005) Cooperative signalling among bacterial chemoreceptors. *Biochemistry* **44:** 14298–14307

Levit MN, Stock JB (2002) Receptor methylation controls the magnitude of stimulus-response coupling in bacterial chemotaxis. *J Biol Chem* **277:** 36760–36765

Li G, Weis RM (2000) Covalent modification regulates ligand binding to receptor complexes in the chemosensory system of *Escherichia coli*. *Cell* **100:** 357–365

Li M, Hazelbauer GL (2004) Cellular stoichiometry of the components of the chemotaxis signalling complex. *J Bacteriol* **186:** 3687–3694

Li M, Hazelbauer GL (2005) Adaptational assistance in clusters of bacterial chemoreceptors. *Mol Microbiol* **56:** 1617–1626

Macnab RM, Koshland Jr DE (1972) The gradient-sensing mechanism in bacterial chemotaxis. *Proc Natl Acad Sci USA* **69:** 2509–2512

Maddock JR, Shapiro L (1993) Polar location of the chemoreceptor complex in the *Escherichia coli* cell. *Science* **259:** 1717–1723

Manson MD, Boos W, Bassford Jr PJ, Rasmussen BA (1985) Dependence of maltose transport and chemotaxis on the amount of maltose-binding protein. *J Biol Chem* **260:** 9727–9733

Manson MD, Kossmann M (1986) Mutations in *tar* suppress defects in maltose chemotaxis caused by specific *malE* mutations. *J Bacteriol* **165:** 34–40

McFall E, Newman EB (1996) Amino acids as carbon sources. In *Escherichia coli and Salmonella: Cellular and Molecular Biology*, Neidhardt FC, Curtiss III R, Ingraham JL, Lin ECC, Low KB, Magasanik B, Reznikoff WS, Riley M, Schaechter M, Umbarger HE (eds), pp 358–379. Washington, D.C: ASM Press

Mello BA, Tu Y (2005) An allosteric model for heterogeneous receptor complexes: understanding bacterial chemotaxis responses to multiple stimuli. *Proc Natl Acad Sci USA* **102:** 17354–17359

Mello BA, Tu Y (2007) Effects of adaptation in maintaining high sensitivity over a wide range of backgrounds for *Escherichia coli* chemotaxis. *Biophys J* **92:** 2329–2337

Mesibov R, Adler J (1972) Chemotaxis toward amino acids in *Escherichia coli*. *J Bacteriol* **112:** 315–326

Mesibov R, Ordal GW, Adler J (1973) The range of attractant concentrations for bacterial chemotaxis and the threshold and size of response over this range. Weber law and related phenomena. *J Gen Physiol* **62:** 203–223

Mowbray SL, Koshland Jr DE (1987) Additive and independent responses in a single receptor: aspartate and maltose stimuli on the tar protein. *Cell* **50:** 171–180

Ordal GW, Adler J (1974) Properties of mutants in galactose taxis and transport. *J Bacteriol* **117:** 517–526

Park S, Wolanin PM, Yuzbashyan EA, Lin H, Darnton NC, Stock JB, Silberzan P, Austin R (2003) Influence of topology on bacterial social interaction. *Proc Natl Acad Sci USA* **100:** 13910–13915

Postma PW, Lengeler JW, Jacobson GR (1993) Phosphoenolpyruvate: carbohydrate phosphotransferase systems of bacteria. *Microbiol Rev* **57:** 543–594

Salman H, Libchaber A (2007) A concentration-dependent switch in the bacterial response to temperature. *Nat Cell Biol* **9:** 1098–1100

Schellenberg GD, Furlong CE (1977) Resolution of the multiplicity of the glutamate and aspartate transport systems of *Escherichia coli*. *J Biol Chem* **252:** 9055–9064

Sourjik V, Berg HC (2000) Localization of components of the chemotaxis machinery of *Escherichia coli* using fluorescent protein fusions. *Mol Microbiol* **37:** 740–751

Sourjik V, Berg HC (2002) Receptor sensitivity in bacterial chemotaxis. *Proc Natl Acad Sci USA* **99:** 123–127

Sourjik V, Berg HC (2004) Functional interactions between receptors in bacterial chemotaxis. *Nature* **428:** 437–441

Sourjik V, Vaknin A, Shimizu TS, Berg HC (2007) *In vivo* measurement by FRET of pathway activity in bacterial chemotaxis. *Methods Enzymol* **423:** 365–391

Strange PG, Koshland Jr DE (1976) Receptor interactions in a signalling system: competition between ribose receptor and galactose receptor in the chemotaxis response. *Proc Natl Acad Sci USA* **73:** 762–766

Yaghmai R, Hazelbauer GL (1993) Strategies for differential sensory responses mediated through the same transmembrane receptor. *EMBO J* **12:** 1897–1905

Zeppenfeld T, Larisch C, Lengeler JW, Jahreis K (2000) Glucose transporter mutants of *Escherichia coli* K-12 with changes in substrate recognition of IICB(Glc) and induction behavior of the ptsG gene. *J Bacteriol* **182:** 4443–4452

Zhang Y, Gardina PJ, Kuebler AS, Kang HS, Christopher JA, Manson MD (1999) Model of maltose-binding protein/chemoreceptor complex supports intrasubunit signaling mechanism. *Proc Natl Acad Sci USA* **96:** 939–944